$$\nu_B = \frac{2n\nu_a}{\lambda_p}$$

Hence, the required *FSR* is given by

$$FSR = \frac{4n\nu_a}{\lambda_p}$$

where ν_a is the acoustic velocity and is ~5.96km/s for silica fibres [4]. For λ_p = 1530.1nm and n = 1.446; *FSR* = 22.5GHz and Δx = 9.2mm, respectively.

Experiment and results: The experimental setup is shown in Fig. 1. The distributed feedback laser source, argon-ion pumped Ti-sapphire system and the erbium-doped fibre amplitier in [1], were replaced by a Q-switched erbium-doped fibre laser (QSL) tunable over 2nm (with centre wavelength of 1530.1nm, spectral width of 1.3GHz, pulse width of 200ns, and a peak power of 200W at 200Hz). The output from the QSL was monitored at photodetector PDI via a 94/6 coupler C1. A 90/10 coupler C2, coupled 30mW into the sensing fibre. The latter consisted of three lengths each of 4.3km (125μm telecommunications grade fibre, specified cut-off of 1180–1280nm, attenuation of <0.22dB). The centre section was placed in an oven and maintained at a temperature of 55°C. The backscattered signal was coupled into the input arm of the MZ via C2.

The MZ was made by connecting together two pairs of arms from two 50/50 couplers, cleaved and polished to the correct length. These formed the cavity arms *X* and *Y* with a path imbalance of 9.2mm. The attenuations in both arms were balanced by placing *Y* in a fibre attenuator (not shown). The Rayleigh and spontaneous Brillouin components were separated into Rayleigh and Brillouin output arms (ROA and BOA, respectively), with each being focused onto 300μm InGaAs photodetectors (PD2 and PD3) connected to a 100MΩ transimpedance amplifier with a post-detection bandwidth of 1MHz. Each detector was connected to a 500MHz digital oscilloscope (Scope) allowing simultaneous viewing of both signals. Signals were averaged 2^{13} times and stored.

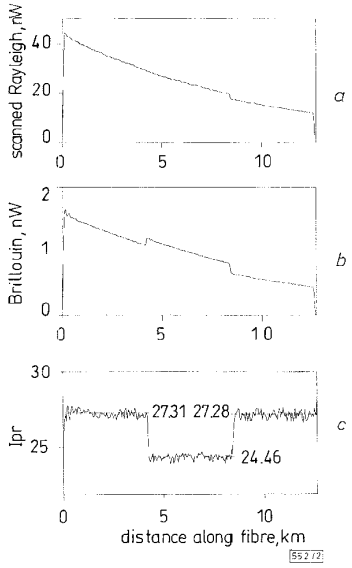

Fig. 2 *Backscatter traces from temperature sensing fibre*

a Scanned Rayleigh
b Brillouin
c LPR

To minimise an impurity Rayleigh signal from entering the BOA, the period of the in-fibre Bragg grating of the QSL was varied thermally by altering the current in an attached peltier cooler. An algorithm was developed which determined the actual Rayleigh impurity in the BOA. Briefly, the algorithm determined the percentage of Rayleigh signal which on subtracting from the Brillouin signal, yielded mimimum coherent Rayleigh noise. It was found that 0.6% of the returning backscattered Rayleigh signal was present in the BOA.

To overcome coherent Rayleigh scattering [5], the QSL was next scanned over 2nm and the backscattered signal in the absence of the MZ was similarly detected, averaged, and stored.

Figs. 2*a*, *b*, and *c* show the graphical results obtained. Fig. 2*a* shows the scanned Rayleigh signal with small perturbations due to coherent Rayleigh scattering, the drop at 86 μs due to a two way splice loss of ~0.4dB. This signal was scaled to the actual Rayleigh signal measured using the MZ. Fig. 2*b* shows the Brillouin signal. Fig. 2*c* shows the Landau-Placzek ratio (LPR). Since the ratio of the LPRs of the heated fibre to the unheated fibre is inversely proportional to the corresponding temperature ratio [1], the temperature in the oven was calculated to be 328.1K for an ambient temperature of 294K. This agrees well with the measured oven temperature of 328K ± 1. A spatial resolution of 40m has been achieved with a temperature resolution of ± 2.9°C.

Conclusion: A novel interferometric technique used in the detection system of a DTS has been demonstrated. The MZ has improved the signal power by a factor of 10 compared to that obtained with a FP. A spatial resolution of 40m as compared to the previously reported 130m has been achieved with a temperature resolution of ± 2.9°C. Moreover, its economical competitiveness, and compact nature makes the MZ ideally suited for this specific technique of distributed temperature sensing. Further refinements of the source and detection systems are currently underway and improved temperature and spatial resolutions are expected shortly.

28 August 1996
Electronics Letters Online No: 19961424

K. De Souza, G.P. Lees, P.C. Wait and T.P. Newson (*Optoelectronics Research Centre, University of Southampton, Southampton SO17 1BJ, United Kingdom*)

E-mail: kds@orc.soton.ac.uk

References

1 WAIT, P.C., and NEWSON, T.P.: 'Landau-Placzek ratio applied to distributed fibre sensing', *Opt. Commun.*, 1996, **122**, (4–6), pp. 141–146
2 LEES, G.P., COLE, M.J., and NEWSON, T.P.: 'Narrow linewidth Q-switched erbium doped fibre laser', *Electron. Lett.*, 1996, **32**, (14), pp. 1299–1300
3 COTTER, D.: 'Stimulated Brillouin scattering in monomode optical fiber', *Opt. Commun.*, 1983, **4**, (1), pp. 10–19
4 AGRAWAL, G.P.: 'Non linear fiber optics' (Academic Press, 1992) p. 372
5 WAIT, P.C., and NEWSON, T.P.: 'Reduction of coherent noise in the Landau Placzek ratio method for distributed temperature sensing measurements', *Opt. Commun.*, (in press)

Optimum gain-equalised configuration of wideband erbium-doped fibre amplifier using inter-stage samarium-doped fibre and midway isolator

Y.K. Chen and S.K. Liaw

Indexing terms: Erbium-doped fibre amplifiers, Fibre amplifiers, Optical fibres

The optimum gain-equalised configuration for the erbium-doped fibre amplifier (EDFA) using a samarium-doped fibre (SDF) is investigated. The dual-pumping scheme with inter-stage SDF and midway isolator was found to be the optimum scheme for obtaining flattened high spectral gain with variation of ≤ ±0.7dB and with a low noise figure of ≤ 5.6dB within the 1530–1560nm range. This amplifier is suitable for multiwavelength transmission systems containing EDFA cascades.

Introduction: Gain-equalisation is one of the major problems facing multiple-channel wavelength-division-multiplexing (WDM) lightwave systems with cascaded erbium-doped fibre amplifiers

(EDFAs). The difficulty in maintaining a flattened gain and an adequate optical signal-to-noise ratio for all channels arises from the non-uniform wavelength-dependent gain profile and saturation characteristics of EDFAs. Many external and intrinsic methods [1 – 5] have been proposed to equalise the EDFA non-uniform spectral gain curve, however, these methods are either complicated or not able to operate properly in the whole 1530–1560nm spectral range. Recently, the authors have reported the feasibility of a simple and passive technique by using a samarium-doped fibre (SDF) as an equaliser [6]. However, the problem of obtaining the optimum gain-equalised configuration using SDF has not yet been addressed. In this Letter, we investigate the optimum configuration of equalised wideband EDFA. It is found that the dual-pumping scheme with inter-stage SDF and a midway optical isolator is the best scheme for achieving flattened high gain with lowest gain variation and low noise figure within the whole EDFA spectral range. This wideband amplifier is suitable for multiwavelength WDM EDFA-repeatered transmission systems and networks.

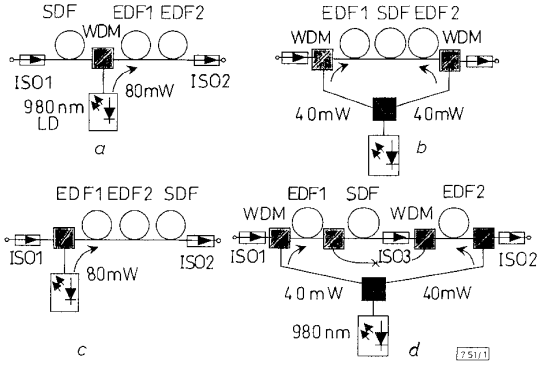

Fig. 1 *Four configurations A, B, C and D of gain-equalised EDFA using samarium-doped fibre (SDF)*

a conf. A
b conf. B
c conf. C
d conf. D

Configurations and experiments: Fig. 1 shows four different configurations (A, B, C and D) of a gain-equalised EDFA with SDF located *a* in front of, *b* between, *c* after, and *d* between, but with the 980nm power-bypassing arrangement and a midway optical isolator, and two segments of the erbium-doped fibres (EDF1 and EDF2), respectively. Both home-made silicate-based EDF and SDF were fabricated by modified chemical vapour deposition (MCVD) and solution soaking techniques [7]. The SDF with an optimal length of 1.5m has an absorption peak of 7.4dB/m at 1525nm with the loss gradually decreased for longer wavelengths

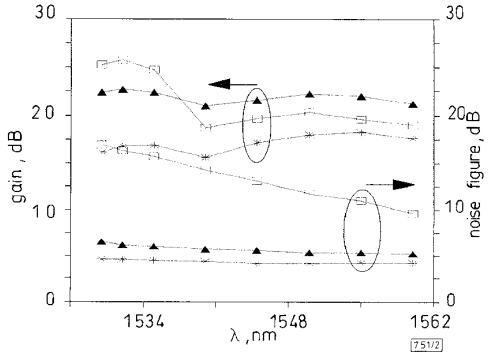

Fig. 2 *Spectral gain and noise figure of gain-equalised EDFAs A, B, and C at input power level of –16 dBm*

□ conf. A
▲ conf. B
✳ conf. C
At *pin* = –16dBm

down to 1.4dB/m at 1565nm. This loss characteristic is suitable for spectral filtering. Each alumino-germano-silicate EDF is 5m in optimal length and 6μm in core diameter, and with a cutoff wavelength of 1120nm and a 5.6dB/m peak absorption at 1532nm. The averaged splicing loss of EDF and SDF was ~0.6dB. The 80mW power from a 980nm pump laser diode was launched into the EDFs via the 980/1550nm WDM couplers in the forward-pumping scheme for confs. A and C, and in the dual-pumping scheme for confs. B and D. The backward-pumping scheme was not considered due to the expected high noise figure (NF) characteristic. To prevent optical reflections, two polarisation-insensitive optical isolators (ISO1 and ISO2) were placed at the input and output ports of the EDFA. The output signal was measured by an optical spectrum analyser and a power meter.

Characteristics and discussions: In the experiments, three configurations, A, B, and C, were first examined with different input power levels. Fig. 2 shows the spectral gain and NF of these amplifiers at an input power level of –16dBm, which is the typical input power level for in-line amplifier cascades. We found that conf. B not only had the most uniform spectral high gain, of 21.4 dB with small gain variation, ΔG, of $\leq \pm 0.7$dB, but also had a fairly low spectral NF of 6.5–5.2dB. Conf. C has moderate uniform gain of 17.1dB with $\Delta G = \pm 1.4$dB and the lowest NF of 4.6–4.2dB. The low gain results from direct superposition of the entire EDFA gain spectrum and the high spectral absorption spectrum of SDF. On the other hand, conf. A has a non-uniform spectral gain with $\Delta G = \pm 3.3$dB and the worst spectral NF of 17–9.6dB, which is due to the high loss of SDF in front of the entire EDFA. Consequently, the dual-pumping scheme, B, with inter-stage SDF has better characteristics of uniform spectral gain and a lower noise figure than that of confs. A and C.

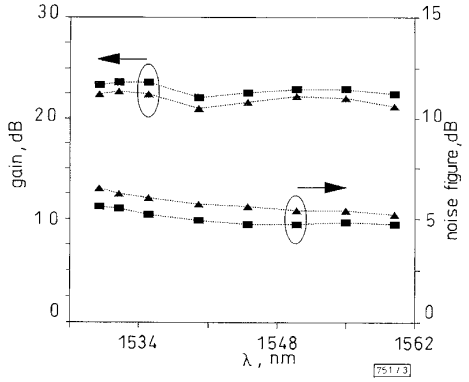

Fig. 3 *Spectral gain and noise figure of gain-equalised EDFA D compared with B at input power level of –16dBm*

▲ conf. B
■ conf. D
At *pin* = –16dBm

To further improve the gain-equalised EDFA, conf. D was arranged and experimented with, from which we found that a rather high absorption loss of ~4.3dB/m at 980nm pump wavelength could not be ignored. In conf. D, two additional inter-stage 980/1550nm WDM couplers were used to avoid absorption of the pump power by the SDF in order to obtain a high pump efficiency. The midway isolator (ISO3) was used to suppress the backward amplified spontaneous emission (ASE) generated by EDF2. Fig. 3 shows the spectral gain and NF of conf. D compared with B at the input power level –16dBm. It was found that conf. D not only has the same spectral gain variation $\Delta G = \pm 0.7$dB, but also has a higher gain of 22.9dB and lower spectral NF of 5.6–4.7dB than that of conf. B. The high gain and low noise figure characteristics are due to (i) two extra inter-staged WDM couplers used to transport 980nm pump power into the EDF on the other side, to maintain high inversion operation, and (ii) the backward ASE was suppressed by the midway isolator. The improved gain and NF differentials are ~1.5 and 0.8dB, respectively.

Conclusions: In conclusion, we have investigated the optimum gain-equalised configuration for a wideband EDFA. We found that the dual-pumping scheme with an inter-stage samarium-doped fibre and a midway isolator is the best scheme for achieving

high gain with least gain variation and the lowest noise figure over the entire 1530–1560nm spectral range. This gain-equalised wideband amplifier may find important applications in multiwavelength WDM transmission systems and networks containing EDFA cascades.

30 September 1996
Electronics Letters Online No: 19961411

Y.K. Chen (*Institute of Electro-Optical Engineering, National Sun Yat-Sen University, PO Box 59-83, Kaoshiung 80424, Taiwan, Republic of China*)

E-mail: ykchen@mail.nsysu.edu.tw

S.K. Liaw (*Institute of Electro-Optical Engineering, National Chiao-Tung University, Hsingchu, Taiwan, Republic of China*)

References

1 CHRAPLYVY, A.R., NAGAL, J.A., and TKACH, R.W.: 'Equalisation in amplified WDM lightwave transmission systems', *IEEE Photonics Technol. Lett.*, 1992, **4**, pp. 920–922
2 ESKILDSEN, L., GOLDSTEIN, E., DA SILVA, V., ANDREFCO, M., and SILBERBERG, Y.: 'Optical power equalization for multiwavelength fibre-amplifier cascades using periodic inhomogeneous broadening', *IEEE Photonics Technol. Lett.*, 1993, **5**, pp. 1188–1190
3 HWANG, S.M., and WILLNER, A.E.: 'Guidelines for optimizing system performance for 20 WDM channels propagating through a cascade of EDFA's', *IEEE Photonics Technol. Lett.*, 1993, **5**, pp. 1190–1193
4 GOLDSTEIN, E., ESKILDSEN, L., LIN, C., and TENCH, R.E.: 'Multiwavelength propagation in lightwave systems with strongly inverted fiber-amplifier', *IEEE Photonics Technol. Lett.*, 1994, **6**, pp. 266–269
5 ALI, M.A., ELREFAIE, A.F., WAGNER, R.E., and AHMED, S.A.: 'Performance of erbium-doped fiber cascades in WDM multiple acccess lightwave networks', *IEEE Photonics Technol. Lett.*, 1994, **6**, pp. 1142–1145
6 LIAW, S.K., and CHEN, Y.K.: 'Passive gain-equalized wideband erbium-doped fiber amplifier using samarium-doped fiber', *IEEE Photonics Technol. Lett.*, 1996, **8**, pp. 879–881
7 TOWNSEND, J.E., POOLE, S.B., and PAYNE, D.N.: 'Solution doping technique for the fabrication of rare-earth doped optical fibres', *Electron. Lett.*, 1987, **23**, pp. 329–331

Reduction of the Shupe effect in fibre optic gyros; the random-wound coil

R.B. Dyott

Indexing terms: Fibre optic gyroscopes, Coils, Windings

A method for reducing the Shupe effect in fibre-optic gyros is described, and verified experimentally. The unbalanced phase shifts in the gyro Sagnac intereferometer that are produced by a traversing temperature gradient are randomised by winding the coil in such a way as to scramble the relative positions of the turns.

Introduction: The Shupe effect [1] is well known as a contributor to drift of the signal in a fibre gyro which is exposed to a change in temperature. It is caused by a temporary phase imbalance in the counter-propagating optical paths of the Sagnac interferometer when a temperature gradient passes through the gyro coil.

A standard solution to the problem is to wind a coil in such a manner that lengths of fibre which are equidistant in phase from the centre of the interferometer are positioned so as to be as close together as possible. One way of achieving this is to use the 'quadrupole' winding [2] which attempts to place the appropriate turns of the coil next to each other. Such a winding needs complicated coil-winding machinery and is not effective at suppressing the Shupe effect equally for every direction from which a temperature gradient can traverse the coil.

Random-wound coil: An alternative solution is to randomise the relative positions of the turns of the coil so completely that there is effectively no resultant phase shift caused by a temperature gradient coming from any direction. However, this condition can never be entirely realised because the coil is 'quantised' by the finite number of turns N. The Shupe effect will instead be diluted by a factor N representing the phase shift due to one turn. The integrated drift over a long period of time (e.g. the time taken for the temperature gradient to pass through the coil) is converted into short term variations with zero mean, which can be represented as 'noise' on the signal. Again, because of the quantum-like nature of the effect, the ratio of 'noise' to signal is further reduced by a factor $N^{1/2}$, making the total reduction in the Schupe effect equal to a factor $N^{3/2}$. This hypothesis has been tested with a computer-driven mathematical model, using a system of random numbers to represent the temperature-induced phase shifts in a random-wound coil. Fig. 1 shows a plot, derived from this model, of $\log_{10}$(noise/signal) against $\log_{10}(N)$. The mean gradient of the line is –1.52, close to the predicted value of –1.5.

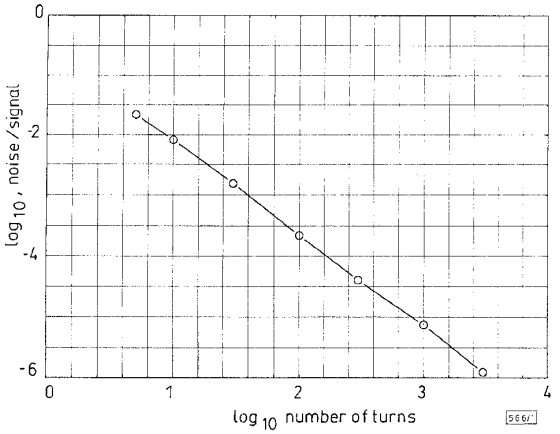

Fig. 1 *Log_{10}(noise/signal) against $log_{10}(N)$ from mathematical model*

Coil winding: It is possible to scramble a winding in the axial direction on a cylindrical former by moving the fibre feed in a random fashion along the coil axis. However, such a coil will always have the fibre at the start of the winding at a smaller radius than that at the end, so that there is no randomisation in the radial direction. One way of achieving randomisation in both axial and radial directions is to wind the fibre as before but on a conical former. The coil is then removed from the former and the conical winding is collapsed to form a flat disc. This scrambles the radial position of the turns and produces a coil which is random both axially and radially. Fig. 2 shows the arrangement.

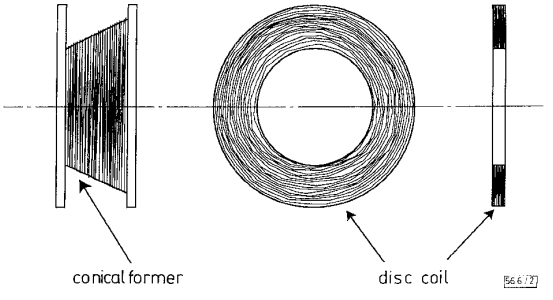

Fig. 2 *Method of construction of random-wound coil*

Experiment: The concept has been tried out using two fibre optic gyros. Both gyros have the following characteristics: Mean diameter of coil: 76.2mm; coil length: 75m; number of turns in coil: 313; source wavelength: 815nm; scource linewidth: 20nm. Gyro *a* has a coil which is randomly wound in the axial direction on a cylindrical aluminium spool which is then incorporated into the gyro. The coil in gyro *b* is randomly wound on a conical former and collapsed to a disc as described. At zero rotation, both gyros are subjected to a positive temperature gradient. The results are shown in Fig. 3. Gyro *a* shows a marked Shupe-induced drift. Undoubtedly the majority of this drift can be attributed to the effect of thermal expansion of the aluminium spool producing circumferential or